DUAL-PILLAR DIELECTRIC LASER ACCELERATION STRUCTURE FOR RELATIVISTIC ELECTRONS

Q.X. Chen[†,1], S. Maru[1], K. Sakaue[1]
[1] The University of Tokyo, Tokyo, Japan

Abstract

Dielectric laser acceleration (DLA) has the potential to provide accelerating gradients on the order of GV/m and is therefore considered a promising alternative to conventional radio-frequency accelerators. Extending DLA operation to relativistic electrons is still at an early stage and is important for realizing compact accelerator systems. In this study, we perform a systematic parameter scan of a top-illuminated fused silica dual-pillar DLA structure to determine the optimal configuration based on electron energy gain. The resulting energy modulation of a relativistic electron bunch is then evaluated using the optimized structure. The simulation results show clear laser-induced energy modulation with an equivalent accelerating gradient on the order of several hundred MV/m. The planned DLA experimental platform at The University of Tokyo linear electron accelerator is also introduced. These results provide guidance for future DLA experiments with relativistic electron beams.

DLA PRINCIPLE AND DESIGN

A grating-based DLA can be regarded as the inverse process of Smith-Purcell radiation [1], as shown in Fig. 1. In the Smith-Purcell effect, an electron passing near a periodic grating emits radiation. In the inverse process, an incident laser excites an evanescent near field at the grating surface. The grating provides the spatial harmonic required to match the optical phase velocity to the electron velocity, producing a longitudinal electric field that can accelerate or decelerate the electron depending on its optical phase. The synchronicity condition is

$$\lambda_g = n\beta\lambda \qquad (1)$$

Where λ_g is the grating period, λ is the laser wavelength, $\beta = v/c$ is the normalized electron velocity, and n is the spatial harmonic order. For the first harmonic and relativistic electrons, this is approximately $\lambda_g = \lambda$.

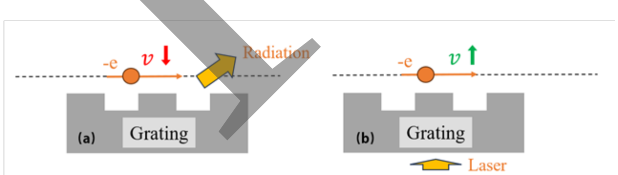

Figure 1: Schematic illustration of the Smith-Purcell effect (a) and inverse Smith-Purcell effect (b).

* Work supported by the MEXT Development of Key Element Technologies to Improve the Performance of Future Accelerators Program, Japan, Grant Number JPMXP1423812204, and JSPS KAKENHI Grant Number 26H02038.
† chenqixin@g.ecc.u-tokyo.ac.jp

Compared with conventional double-grating DLA structures, the dual-pillar geometry offers a simpler and more flexible platform for beam manipulation, while avoiding the mechanical alignment difficulty between two separated gratings [2]. It can also support symmetric optical-field excitation in the channel and can be configured for acceleration, focusing, bunching, or beam steering.

As shown in Fig. 2, three typical illumination schemes can be used for a dual-pillar DLA: double-sided illumination, single-sided illumination with a Bragg reflector, and top illumination. Double-sided illumination can provide the highest field symmetry in the acceleration channel, but it requires precise spatial, temporal, and phase alignment of two incident laser pulses. Single-sided illumination simplifies the optical system by using only one drive laser; however, without perfect compensation from the reflector, the excited field can become asymmetric in the channel, which may introduce unwanted transverse effects. Top illumination further simplifies the optical layout and relaxes the alignment requirements [2, 3]. Although this configuration may provide a slightly lower maximum accelerating field than the other schemes, it offers the best simplicity and feasibility for experimental implementation and future applications, including multi-channel operation and on-chip integration.

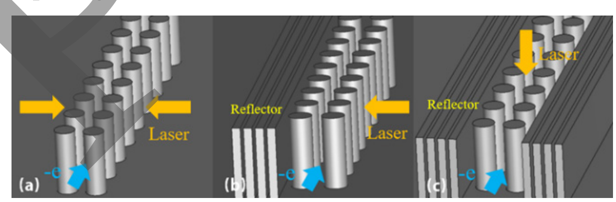

Figure 2: Illumination schemes for a dual-pillar DLA: (a) dual-sided, (b) single-sided with a Bragg reflector, and (c) top illumination.

In this study, a laser wavelength of λ = 1950 nm is used for both simulations and future experiments. Fused silica is selected as the baseline material for the DLA structure because its laser damage threshold is nearly one order of magnitude higher than that of silicon [4, 5]. This allows higher incident laser fields and makes it possible to reach accelerating gradients of several hundred MV/m. Since the interaction length of the proposed structure is limited [6, 7], a high accelerating gradient is required to obtain a measurable energy gain, especially for high-energy electron beams where a clear energy modulation signal is needed.

SIMULATION RESULTS

The geometric parameters of the top-illuminated dual-pillar DLA structure are optimized using CST Studio Suite. The simulation model is shown in Fig. 3. The electron beam propagates along the longitudinal z-direction through the center of the channel, while the drive laser is incident from the top of the structure. Each pillar has an elliptical cross section, with D_z and D_x denoting the longitudinal and transverse dimensions respectively. The lower panels of Fig. 3 show the longitudinal electric field E_z in the acceleration channel at two representative optical phases, illustrating the phase reversal of the accelerating field during one optical cycle. A two-dimensional parameter scan of D_z and D_x is performed with a step size of 0.1λ.

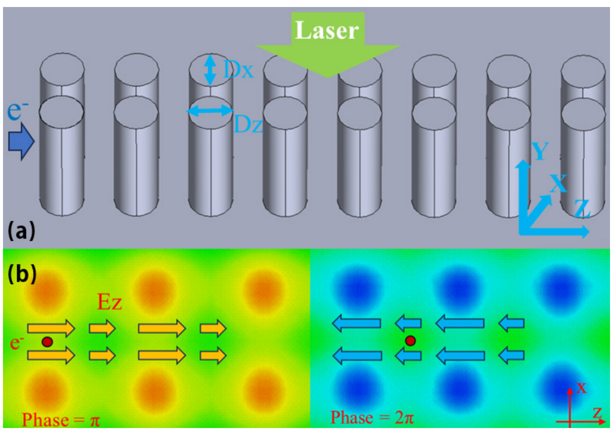

Figure 3: Simulation model of the top-illuminated dual-pillar DLA (a) and E_z field distribution (b).

For each geometry, a phase-matched electron passing through the channel center is tracked, and the maximum energy gain is used to evaluate the acceleration performance. The resulting parameter map is shown in Fig. 4.

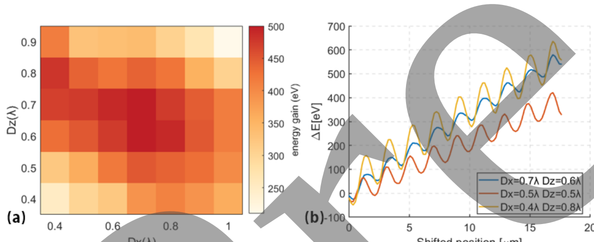

Figure 4: Parameter scan result (a) and comparison of energy gain results for selected parameter sets (b).

In the parameter map shown in Fig. 4(a), darker colors indicate larger electron energy gain. The maximum energy gain is obtained at $D_x = 0.7\lambda$ and $D_z = 0.6\lambda$, indicating that the structure is close to the optimized geometry under the present simulation conditions. Fig. 4(b) shows the electron energy-gain evolution for several representative sets of structural parameters. The oscillatory behavior of the energy gain curves indicates that the electron experiences both accelerating and decelerating phases within each structure period. Under the optimized parameter set, for an incident laser field of approximately 400 MV/m, the electron gains about 500 eV over eight structure periods, corresponding to an equivalent accelerating gradient of 32 MV/m.

The calculated electric field distribution is imported into General Particle Tracer (GPT) for particle tracking simulations. The initial bunch is modelled as a Gaussian distribution truncated at 4σ in all three spatial dimensions and in energy, with a relative energy spread of 0.05% and an initial angular divergence of 0.5 mrad. The longitudinal bunch length is set to 16 μm, corresponding to approximately 53 fs, or about eight optical cycles at λ = 1950 nm. This shortened bunch length, compared with the expected experimental value of several hundred femtoseconds, is chosen to resolve the spatial phase evolution in the DLA channel and to provide an intuitive view of the phase-dependent beam dynamics.

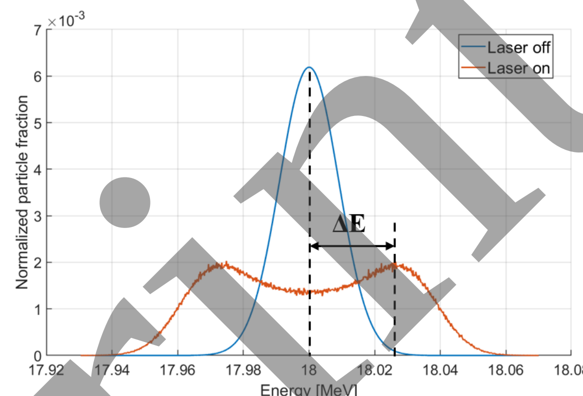

Figure 5: Simulated energy modulation of the electron bunch before and after DLA interaction.

For an incident laser field of 6 GV/m, the simulated electron energy distribution before and after the DLA interaction is shown in Fig. 5. Although the bunch length covers several optical periods, each longitudinal slice of the bunch remains phase-matched to the corresponding accelerating or decelerating phase of the laser-driven near field. As a result, electrons at different phases experience different energy changes, and the DLA effect appears mainly as an energy modulation rather than a uniform shift of the whole bunch energy. After passing through 24 structure periods, corresponding to an interaction length of approximately 45 μm, the maximum energy modulation reaches about 25 keV. The corresponding equivalent accelerating gradient is approximately 500 MV/m, in good agreement with the single-electron energy gain result calculated in CST.

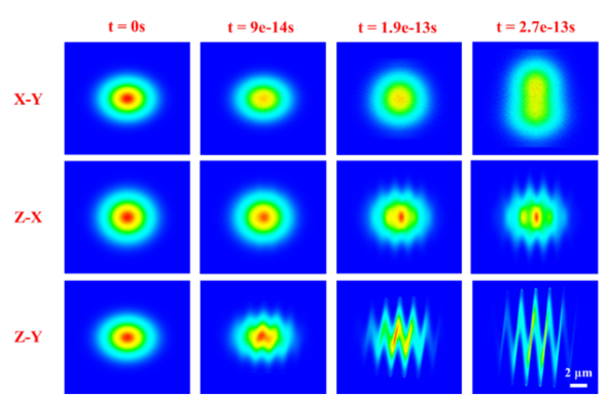

Figure 6: Projected electron bunch density evolution during the DLA process.

Figure 6 shows the time evolution of the projected electron bunch density in the x-y, z-x, and z-y planes during the DLA interaction. In the transverse x-y plane, the bunch profile remains relatively stable in the x-direction, while a noticeable expansion appears along the y-direction. In the z-x plane, a periodic density modulation is observed, but the modulation amplitude is relatively small, indicating that the x-component field has only a limited influence on the bunch distribution. In contrast, the z-y plane shows a strong periodic density modulation, suggesting a non-negligible y-component field and a stronger transverse effect on the electron bunch.

This behavior differs from previously reported results for silicon-based dual-pillar structures. In the fused-silica structure studied here, the transverse modulation is more pronounced in the y-direction, whereas the distortion in the x-direction remains relatively weak. This trend is opposite to that reported for silicon structures and may be related to the large difference in refractive index, which modifies the near-field distribution in the acceleration channel [8, 9]. Further investigation is needed to clarify this mechanism, since such transverse fields may affect beam transport in long-range DLA process.

EXPERIMENTAL PLAN

The experimental platform for the planned DLA beam acceleration test is currently under construction. The experiment will be carried out using the linear electron accelerator of the University of Tokyo, located at Tokai, Ibaraki. Electron bunches are generated by a photocathode RF gun and subsequently accelerated in the linac. Figure 7 shows photographs of the RF gun section and the main accelerator beamline, which will serve as the electron source for the future DLA experiment.

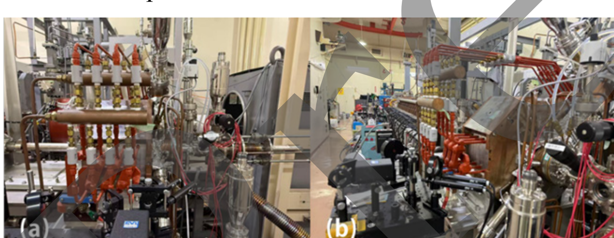

Figure 7: Photographs of the photocathode RF gun (a) and linac beamline (b) at The University of Tokyo.

As shown in Fig. 8, the DLA structure will be installed in a dedicated vacuum chamber located downstream of the acceleration section. Since the experimental station is currently under construction, the vacuum chamber and laser transport line are still being designed. In the present baseline configuration, a 1 ps laser pulse with a central wavelength of 1950 nm will be delivered to the DLA interaction point and coupled to the dielectric structure. The laser-driven near field excited in the structure will interact with the 18 MeV electron beam. After the DLA interaction, the dispersed beam image will be recorded on a scintillator screen using a high-speed camera. The acceleration effect will be evaluated from the laser-induced energy modulation by comparing the energy spectra with and without laser input to the DLA structure.

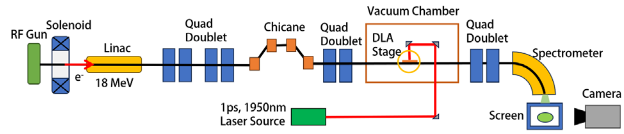

Figure 8: Schematic layout of the planned DLA experimental platform.

CONCLUSIONS

In this work, a top-illuminated fused silica dual-pillar DLA structure was designed and numerically investigated for relativistic electron acceleration. The optimized geometry was obtained at $D_x = 0.7\lambda$ and $D_z = 0.6\lambda$ from the parameter scan. Under an incident laser field of approximately 400 MV/m, a phase-matched electron gained about 500 eV over eight structure periods, corresponding to an equivalent accelerating gradient of 32 MV/m. Particle tracking simulations were then performed for an 18 MeV electron bunch with a relative energy spread of 0.05%. For an incident laser field of 6 GV/m, the bunch showed an energy modulation of about 25 keV after 24 structure periods, corresponding to an equivalent accelerating gradient of approximately 500 MV/m. The projected density evolution indicated a non-negligible transverse field effect in the y-direction, which may influence beam transport in long-range DLA acceleration. The planned beam-test platform at the University of Tokyo linear electron accelerator was also introduced. The present results provide guidance for future fused silica DLA experiments with relativistic electron beams.

REFERENCES

[1] R. J. England *et al.*, "Dielectric laser accelerators", *Rev. Mod. Phys.*, vol. 86, no. 4, pp. 1337-1389, 2014. doi:10.1103/revmodphys.86.1337

[2] R. Shiloh *et al.*, "Miniature light-driven nanophotonic electron acceleration and control," *Adv. Opt. Photonics*, vol. 14, no. 4, p. 862, Dec. 2022. doi:10.1364/aop.461142

[3] R. Shiloh, T. Chlouba, P. Yousefi, and P. Hommelhoff, "Particle acceleration using top-illuminated nanophotonic dielectric structures," *Biomed. Opt. Express*, vol. 29, no. 10, p. 14403, Apr. 2021. doi:10.1364/oe.420235

[4] A.-C. Tien, S. Backus, H. Kapteyn, M. Murnane, and G. Mourou, "Short-Pulse Laser Damage in Transparent Materials as a Function of Pulse Duration," *Phys. Rev. Lett.*, vol. 82, no. 19, pp. 3883–3886, May 1999. doi:10.1103/physrevlett.82.3883

[5] K. Soong, R. L. Byer, E. R. Colby, R. J. England, and E. A. Peralta, "Laser damage threshold measurements of optical materials for direct laser accelerators," in *15th Advanced Accelerator Concepts Workshop*, Ed., 2013, pp. 511–515. doi:10.1063/1.4773749

[6] S. Crisp, A. Ody, J. England, and P. Musumeci, "Extended interaction length laser-driven acceleration in a tunable dielectric structure," *Phys. Rev. Accel. Beams*, vol. 27, no. 5, May 2024. doi:10.1103/physrevaccelbeams.27.051303

[7] D. Cesar *et al.*, "Enhanced energy gain in a dielectric laser accelerator using a tilted pulse front laser," *Biomed. Opt. Express*, vol. 26, no. 22, p. 29216, Oct. 2018. doi:10.1364/oe.26.029216

[8] T. Chlouba, R. Shiloh, S. Kraus, L. Brückner, J. Litzel, and P. Hommelhoff, "Coherent nanophotonic electron accelerator," *Ann. Sci. Nat. Zool. Biol. Anim.*, vol. 622, no. 7983, pp. 476–480, Oct. 2023. doi:10.1038/s41586-023-06602-7

[9] K. J. Leedle *et al.*, "Dielectric laser acceleration of sub-100 keV electrons with silicon dual-pillar grating structures," *Opt. Lett.*, vol. 40, no. 18, p. 4344, Sep. 2015. doi:10.1364/ol.40.004344